STRESS ANALYSIS AND STABILITY OF COMPOSITE CYLINDERS SUBJECTED TO COMBINED LOADS

Flamínio Levy-Neto, flaminio@unb.br
Taygoara Felamingo de Oliveira, taygoara@unb.br
UnB – FT – ENM, Departament of Mechanical Engineering, 70910-900 – Brasilia – DF

Abstract. *The main objective of this work is to present numerical results concerned with the influence of the winding angle ($\pm\theta$), on the elastic stability and the strength of composite cylinders, closed at both ends and subjected to combined internal pressure and axial compression. The cylinders analyzed in this investigation were composed of stacked layers of epoxy resin reinforced with: (i) E-glass; and (ii) carbon fibers, forming angle ply laminates, with $\pm 20^\circ \leq \theta \leq \pm 90^\circ$. In all the simulations, using the finite element method, the axial load consisted of a longitudinal pressure, eight times higher than the lateral pressure (i.e. 8 x p). The final failure of the models was controlled either by bifurcation buckling (i. e. loss of stability) or by material failure (i.e. fracture os the composite layers). In the simulations, the most critical mode of failure was bifurcation buckling, with the number of circumferential waves varying from 2 to 4. For the models reinforced with E-glass the minimum buckling pressures occurred for $\theta = \pm 20^\circ$ and the maximum for $\theta = \pm 90^\circ$ (i.e. hoop winding). For those reinforced with carbon the maximum bucking pressure occurred for $\theta = \pm 62.8^\circ$ and the minimum for $\theta = \pm 20^\circ$.*

Keywords*: composite cylinders, elastic stability*

1. INTRODUCTION

Structures designed to withstand internal water pressure, combined with high axial compressive loads, usually appear in the form of thin-walled curved shells constructed from metals and composites. The use of Fibre Reinforced Plastic (FRP) pipes in marine structures, as an alternative to metallic materials, is attractive from the points of view of weight saving and corrosion-strength (Daniel and Ishai, 2006). However, it is only recently that extensive experimental and numerical results concerned with the behaviour and failure modes of internally pressurised FRP pipes, with additional axial compression, have been reported in the literature (Hoa, 1999). These studies indicated that, depending on the geometry of the cylinder and the nature of the reinforcing fibres, there are at least 3 possible modes of failure, or final collapse, for FRP composite cylinders subjected to axial compression (Campestrini, 1997; Baldoino, 1998; and Gonçalves et al., 2001):
(i) bifurcation buckling (BB) or axisymmetric collapse (AC), for thin cylinders reinforced with E-glass and S-glass fibers, as illustrated in Figure 1;
(ii) material failure controlled by First Ply Failure (FPF), for moderately thicker shells reinforced either with carbon or E-glass; and
(iii) material failure controlled by Last Ply Failure (LPF), for thicker cylinders reinforced with more than 10 layers of carbon fabrics.

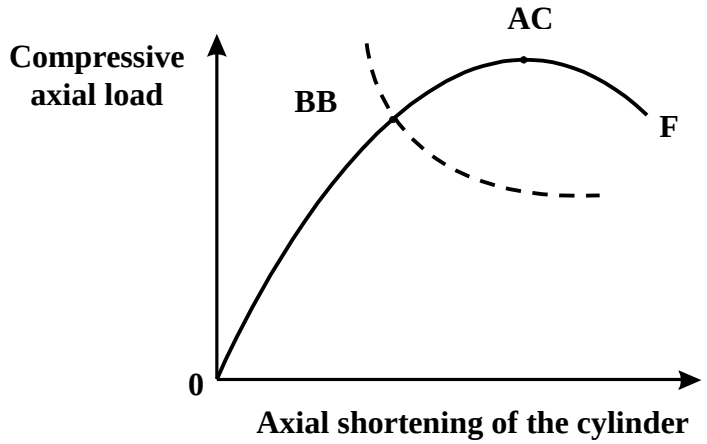

Figure 1. Fundamental and secondary load paths for a cylinder subjected to a compressive axial load

The axissimetrical collapse (AC) takes place when a perfect cylinder, subjected to axial compression loads (e.g. uniform external pressure applied to the flat ends), looses its stiffness completely and a global collapse occurs. The bifurcation buckling (BB), on the other hand, is a more localized instability associated with circumferential waves and normally occurs

when the shell has some sort of geometrical imperfection (Ross, 1990). In addition, the onset of BB is associated with a change, from the fundamental to a secondary load path, represented by the dotted line shown in Figure 1. So, at a particular load along the fundamental path, there is a bifurcation towards the secondary path. The instabilities related to AC and BB normally takes place when the cylinder is thin and presents an elevated ratio of radius (R) over wall thickness (t), R/t. On the other hand, if the ratio R/t decreases, material failure can take place before AC and BB. If the laminated shell has few composite plies, the material failure can be controlled by first ply failure, FPF. And, if the number of layers increases, eventually, the failure can be controlled by last ply failure, LPF (Tsai, 1987; Gibson, 1996; Daniel and Ishai, 2006).

Since composite pressure vessels and submersible structures are being be used in off shore petroleum platforms, in particular those localized in deep waters, theoretical and experimental studies in this field are important. However, experimental work in the area of composite submersible structures is complex and very expensive (Hoa, 1999, Gonçalves, 2001). In this scenario, many theoretical studies are developed in the first place, to gather information and even to predict the mechanical behavior of composite shells, before an experimental investigation takes place. Even though, the number of publications concerned with theoretical studies in this field is also reduced. In view of the limited number of published results in this field, particularly in Brazil, the aim of this numerical study was to investigate the behavior of FRP cylindrical shells with total length L = 800 mm, diameter D = 200 mm, nominal thickness t = 2mm, as shown in Figure 2. In this case, since R / t = 50, the composite shell can be considered thin (Ross, 1990; and Levy Neto, 1991).

2. SCOPE OF THE STUDY

All the cylinders simulated in this work had a nominal diameter of 200 mm, total length over diameter ratio L/D = 4 and the shell wall consisted of an angle-ply laminate (i.e. stacking sequence [+ θ / - θ]) of six unidirectional laminae, of 0.33 mm each, totalizing t = 2mm. The epoxy resin was adopted as matrix for the models, and both, carbon (T 300) and E-glass fibers were used as unidirectional reinforcement. The mechanical properties of these materials are presented in Tables 1 and 2. So, two groups of composite cylinders were simulated. In both groups, the orientation of the fibers varied from ± 20° to ± 90°. The models were closed at both ends with circular steel flat plates and subjected to combined axial compression and internal pressure (p). The axial load was obtained applying an uniform external pressure, eight times larger than the internal pressure (i.e. 8 * p), on the surface of the flat ends. The simulations were based on a non linear finite element program for axissimetric shells, in which the only element is a ring, with two nodes and each node has four degrees of freedom (u, v, w and β), as shown in Figure 3. More details concerned with the program are presented in section 3. The coordinate X is axial, R is radial and S runs along a meridian, on the surface of the shell wall.

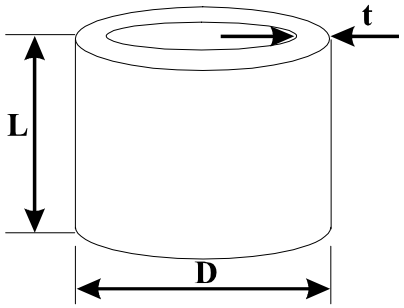

Figure 2 . Geometry of the cylinders

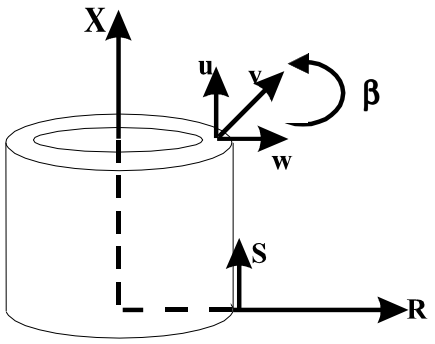

Figure 3 . Degrees of freedom of the ring element

Table 1 . Mechanical properties of the E-glass/epoxy lamina (Tsai, 1987).

Mechanical properties of the E-glass/epoxy lamina	
Specific mass, ρ (g/cm^3)	1.9
Longitudinal Elasticity Modulus, E_{11} (GPa)	38.60
Transversal Elasticity Modulus, E_{22} (GPa).	8.27
Minor Poisson's ratio	0.06
In plane shear modulus G_{12} (GPa)	4.14
Longitudinal tensile strength, X_{1T} (MPa)	1062
Transversal tensile strength X_{2T} (MPa)	31
Longitudinal compressive strengthX_{1C} (MPa)	610
Transversal compressive strength, X_{2C} (MPa)	118
Shear strength, S_{12} (MPa)	72

The relevant elastic and strength properties of the FRP plies used in this investigation, including: the Elasticity Moduli along the directions parallel and perpendicular to the fibers, E_1 and E_2; the Shear Modulus, G_{12}; the Poisson Ratio, ν_{12}; the ultimate strengths in tension, X_{1T} and X_{2T}; the ultimate strengths in compression, X_{1C} and X_{2C}; and the shear strength, S_{12}, are presented in Tables 1 and 2.

Table 2 . Mechanical properties of the carbon/epoxy lamina (Tsai, 1987).

Mechanical properties of the carbon/epoxy lamina	
Specific mass, ρ (g/cm^3)	1.6
Longitudinal Elasticity Modulus, E_{11} (GPa)	181.0
Transversal Elasticity Modulus, E_{22} (GPa).	10.3
Minor Poisson's ratio	0.016
In plane shear modulus G_{12} (GPa)	7.17
Longitudinal tensile strength, X_{1T} (MPa)	1500
Transversal tensile strength X_{2T} (MPa)	40
Longitudinal compressive strength, X_{1C} (MPa)	1500
Transversal compressive strength, X_{2C} (MPa)	246
Shear strength, S_{12} (MPa)	68

The flat ends used to close the cylinders were assumed to be made of low carbon steel, presenting Elasticity Modulus E = 200 GPa, Poisson ratio ν = 0.3 and yield stress σ_y = 300 MPa.

3. THEORETICAL MODELLING

Three failure modes of the FRP laminated cylinders were considered in the theoretical analysis (i.e. BB, AC and FPF). In those, the laminated composite shell wall was treated as a layered orthotropic material, according to the Classical Laminated Theory (Hull and Clyne, 1996; Daniel and Ishai, 2006).

Initially, an "in-house" finite element program for orthotropic axisymmetric shells (COMPSHELL, Levy Neto, 1991; Gonçalves et al., 2001) was developed to predict both the stability (BB or AC) and the material failure (FPF, only) pressures of the models. The program COMPSHELL is a finite element code based on a two nodes ring element, in which the shell wall can be made of orthotropic layers, and each node has four degrees of freedom, three displacements (u, v, and w) and one meridian rotation (β), as illustrated in Figure 3. The bifurcation buckling BB, or structural stability, condition was obtained when the second variation of the total strain energy of the system vanishes. This condition is established by a combination of step-by-step search and eigenvalue analysis. In order to calculate the FPF pressures the quadratic failure criteria of Tsai-Hill and Hoffman, presented in Eqs. (1) and (2), were adopted. These criteria, based on the in-plane stresses of all the FRP layers of the composite wall, were used for all the nodal points in the finite element mesh. More details concerned with the theoretical predictions of the collapse pressures can be found in the work of Levy Neto (1991).

The boundary conditions of the simulated models, clamped at the base and free to present longitudinal displacements (u) at the top flat end, are illustrated in Figure 4. The coordinate S, which runs along a meridian on the surface of the shell wall, has its origin at the clamped edge of the cylinder.

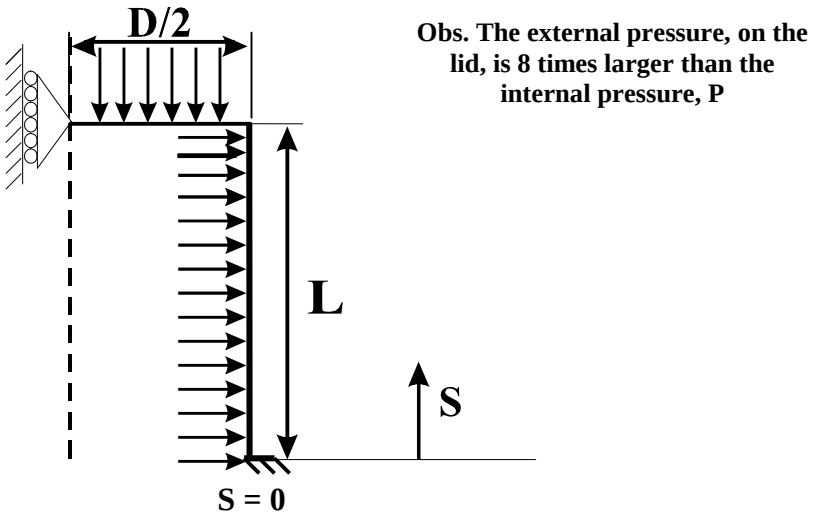

Figure 4 . Boundary conditions for the simulated cylinders

In order to evaluate if the material failure of the FRP composite layers takes place, or not, when subjected to in plane bidimensional stresses, the failure criteria of Tsai Hill and Hoffman for orthotropic laminae were adopted (Daniel and Ishai, 2006). These criteria are based on quadratic equations, as illustrated in Eqs. (1) and (2):

$$\left(\frac{\sigma_1}{X_1}\right)^2 - \frac{\sigma_1 \cdot \sigma_2}{X_1^2} + \left(\frac{\sigma_2}{X_2}\right)^2 + \left(\frac{\tau_{12}}{S_{12}}\right)^2 = 1. \qquad (1)$$

where: $X_1 = X_{1T}$ or X_{1C} and $X_2 = X_{2T}$ or X_{2C}, depending on the sign of the normal applied in plane normal stresses: σ_1, parallel to the fibers; and σ_2 , perpendicular to the fibers. For $\sigma_1 > 0$, the tensile strength is used and for σ_1 , < 0 , the compressive strength is used. The same occurs for σ_2 . τ_{12} is the in plane applied shear stress and the in plane shear strength is S_{12}. When the left side of Eq. 1 is equal to 1, this means that the lamina is in the threshold of failure. If the left side is smaller than 1 the lamina do not fail (Daniel and Ishai, 2006). The failure theory of Hoffman has quadratic and linear terms combined, as shown in Eq. (2):

$$\sigma_1 \cdot F_1 + \sigma_2 \cdot F_2 + \sigma_1^2 \cdot F_{11} + \sigma_2^2 \cdot F_{22} + \tau_{12}^2 \cdot F_{33} + 2 \cdot \sigma_1 \cdot \sigma_2 \cdot F_{12} = 1; \qquad (2)$$

where: $F_1 = \frac{1}{X_{1T}} - \frac{1}{X_{1C}}$; $F_2 = \frac{1}{X_{2T}} - \frac{1}{X_{2C}}$; $F_{11} = \frac{1}{X_{1T} \cdot X_{1C}}$;

$F_{22} = \frac{1}{X_{2T} \cdot X_{2C}}$; $F_{33} = \frac{1}{S_{12}^2}$; and $F_{12} = -\frac{1}{2 \cdot X_{1T} \cdot X_{1C}}$.

The coeficients of the failure criterion of Hoffman, F_1 , F_2 , F_{11} , F_{22} , F_{33} and F_{12} are related to the lamina strengths, according to the relations presented above (Daniel and Ishai, 2006).

4. MAIN RESULTS

4.1. First Ply Failure (FPF) pressures P, of the cylinders under combined axial and lateral loads.

For the cylinders reinforced with six E-glass/epoxy layers, with total length L = 800 mm, L/D = 4 and D/t = 100, when the winding angles varied from ± 20° to ± 90°, at increments of 5°, the numerical results for the FPF strength (First Ply Failure pressure, P, at which material failure occurs) of the models are presented in Figure 5. The cylinder is subjected to combined loads in which P is the internal (or lateral) pressure and Pe = 8 . P is an external pressure, applied on the lids, subjeting the cylinder to a simulteneos axial compression, as illustrated in Figure 4.

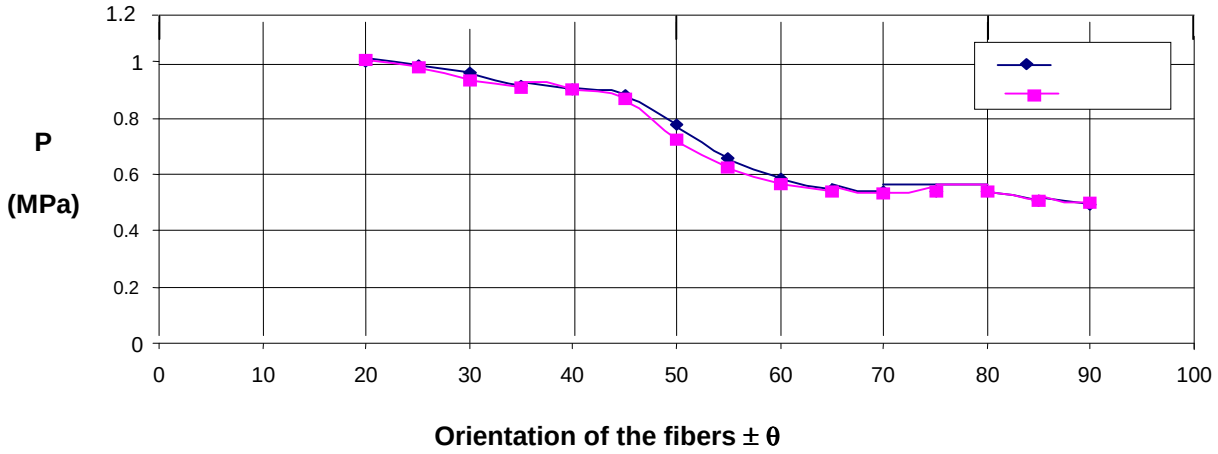

Figure 5 . FPF pressures for the E – glass/eopxy cylindres for 20° < ± θ < 90°

The same simulations were carried out for the cylinders reinforced with six carbon/epoxy layers, which were subjected to the same boundary conditions (see Fig. 4) and present the same geometry of the E-glass/epoxy ones: total thickness t = 2 mm; L = 800 mm and D = 200 mm. The numerical results for the FPF strength (First Ply Failure pressure, P, at which material failure occurs) of the carbon/epoxy models are presented in Figure 6.

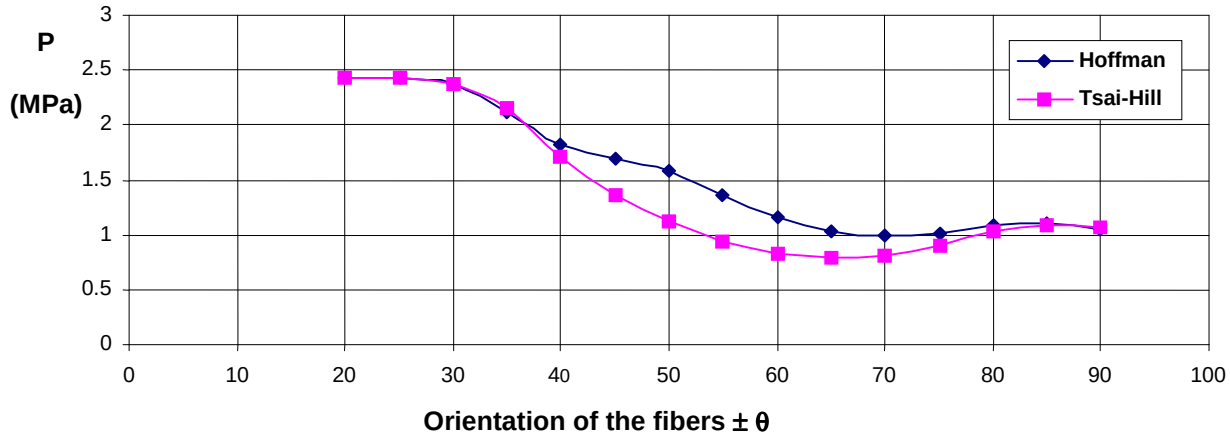

Figure 6 . FPF pressures P for the carbon /eopxy cylindres, for 20° < ± θ < 90°

4.2 . Buckling pressures, Pb, of the cylinders under combined axial and lateral loads.

In addition to the calculation of the FPF pressures of the cylinders reinforced with E-glass and carbon fibers, based on the failure criteria of Hoffman and Tsai-Hill, the buckling pressures, Pb, for these models were also obtained using the program COMPSHELL. These results are presented in Figures 7 and 8, respectively.

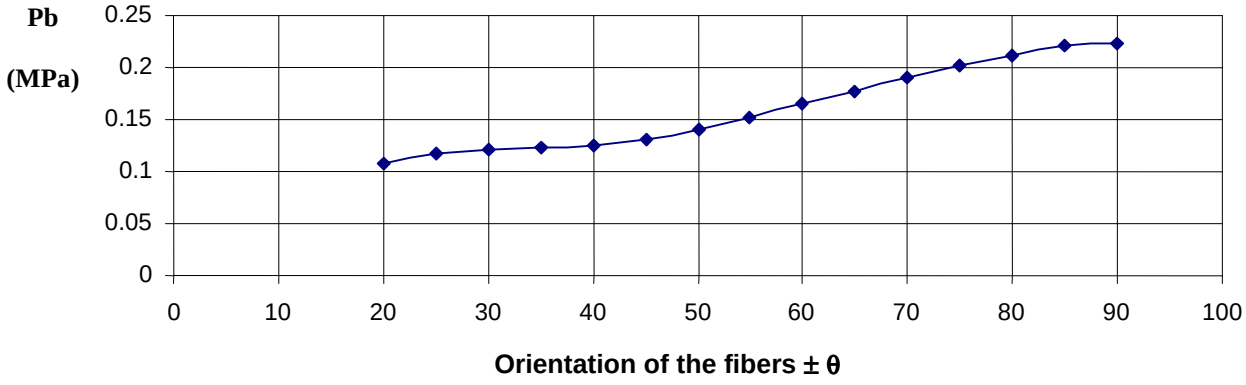

Figure 7 . Buckling pressures Pb of the E-glass/epoxy cylinders, for 20° < ± θ < 90°

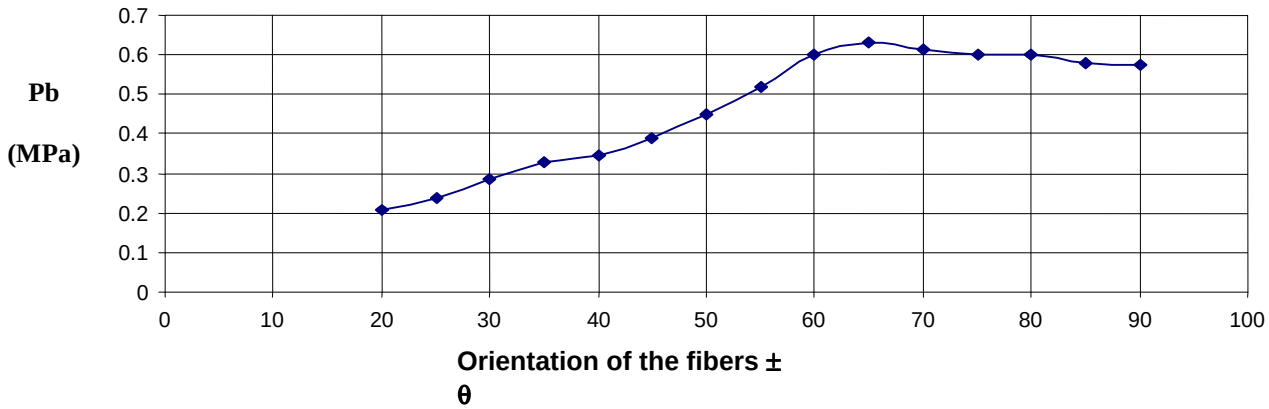

Figure 8 . Buckling pressures Pb of the carbon/epoxy cylinders, for 20° < ± θ < 90°

The buckling pressures Pb are associated to the number of circumferential waves (n) of the buckling mode, which presents the minimum failure pressure for each angle of orientation for the reinforcing fibers. These information's, for both cylinders, are presented at Tables 3 and 4. Figure 8 indicates that the maximum buckling pressure, Pb, of the carbon/epoxy cylinders occurs in the range of orientation of fibers between $60° < \pm \theta < 70°$. So, in order to obtain more precise results, the calculations presented in Figure 8 were refined many times over in this particular range and are presented in Figure 9. The refined calculations indicate that the optimum orientation of the carbon fibers, for maximum buckling pressure is $\pm$ 62.8 °, and this failure mode (elastic bifurcation buckling) is associated with two (2) circumferential waves.

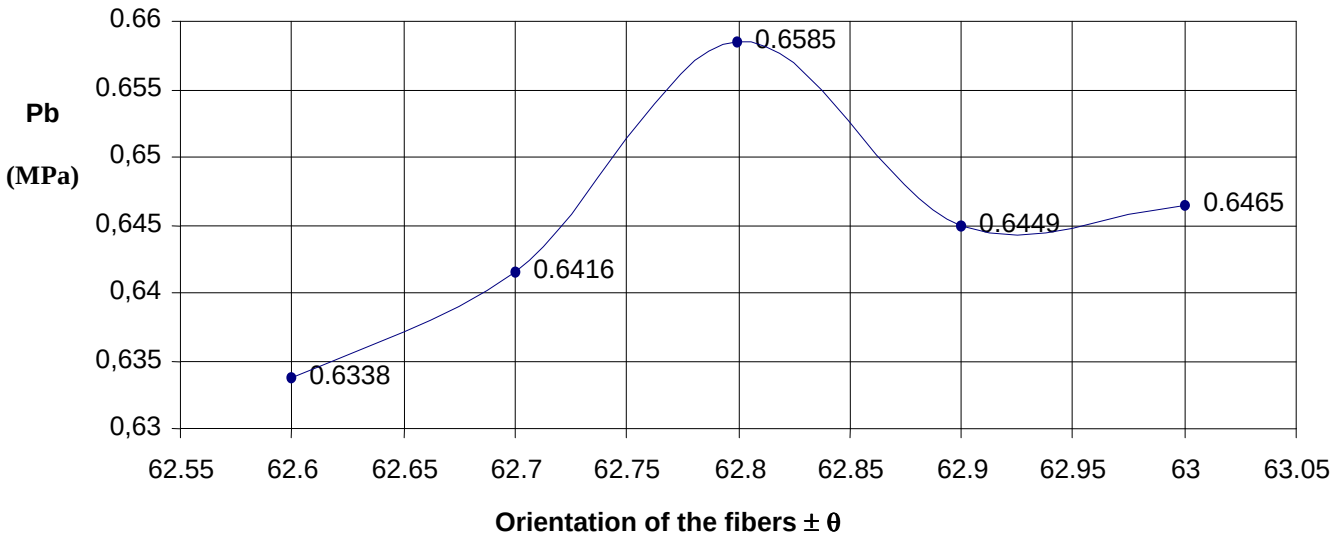

Figure 9 . Buckling pressures Pb of the carbon/epoxy cylinders, for $62.6° < \pm \theta < 63°$

Table 3 . Buckling pressures Pb of the E-glass/epoxy cylinders, for $20° < \pm \theta < 90°$, associated with the correspondent number of circumferential waves.

Orientation of the fibers ± θ °	Buckling pressure, Pb (MPa)	Nº of circumferential waves
20°	0.1081	4
25°	0.1165	4
30°	0.1221	3
35°	0.1223	3
40°	0.1255	3
45°	0.1308	3
50°	0.1407	3
55°	0.1525	3
60°	0.1652	3
65°	0.1777	3
70°	0.1897	3
75°	0.2013	3
80°	0.2123	3
85°	0.2219	3
90°	0.2229	3

Table 3 indicates that the variation of the number of circumferential waves, from 3 to 4, is not significant. But, on the other hand, the sensitivity of the buckling pressure (Pb) with the orientation of the fibers is very intense. In particular, for $\theta = \pm 20°$ Pb = 0.1081 MPa, whereas for $\theta = \pm 90°$ Pb = 0.2229 MPa, which is a variation of about 106%.

Table 4 . Buckling pressures Pb of the carbon/epoxy cylinders, for $20° < \pm \theta < 90°$, associated with the correspondent number of circumferential waves.

Orientation of the fibers ± θ °	**Buckling pressure, Pb (MPa)**	**Nº of circumferential waves**
20°	0.2057	4
25°	0.2372	4
30°	0.2864	4
35°	0.3271	3
40°	0.3475	3
45°	0.3889	3
50°	0.4481	3
55°	0.5198	3
60°	0.5985	3
65°	0.6299	2
70°	0.6138	2
75°	0.6021	2
80°	0.6021	2
85°	0.5802	2
90°	0.5740	2

For the carbon/epoxy cylinders, the variation of the number of circumferential waves, from 2 to 4, as shown in Table 4, is more significant, in comparison with the E-glass/epoxy models. And, in addition, the sensitivity of the buckling pressure (Pb) with the orientation of the fibers, for the carbon/epoxy cylinders is even more intense. In particular, for $\theta = \pm 20°$ Pb = 0.2057 MPa, whereas for $\theta = \pm 90°$ Pb = 0.5740 MPa, which is a variation of about 179%.

5. DISCUSSION OF THE RESULTS

For the E-glass/epoxy cylinders subjected to axial compression and internal pressure, it is clear from the results obtained in the simulations (see Figures 5 and 7, as well as Table 3) that the bifurcation buckling (BB) occurs at lower pressures than First Ply Failure (FPF). The failure pressures, P, for FPF, were all above 0.5 MPa, for $20° < \pm \theta < 90°$, whereas, the buckling pressures, Pb, varied from 0.1081 MPa, for $\pm \theta = 20°$, to 0.2229 MPa, for $\pm \theta = 90°$. Similar behavior also took place for the carbon/epoxy cylinders, where the FPF pressures, P, were all above 0.7 MPa and the BB pressures, Pb, varied from 0.2057 MPa for $\pm \theta = 20°$, to 0.5740 MPa, for $\pm \theta = 90°$. .

The geometry of the specimens, including total length, diameter and thickness, is exactly the same for both cylinders. So, in this scenario, for $20° < \pm \theta < 90°$, the simulations indicate that the buckling pressures of the carbon/epoxy models are, at least, about two times higher, and the FPF strengths about 40% higher, relativelly to those presented by the E-glass/epoxy cylinders.

Both, the bifurcation buckling (BB) pressures, Pb, and the FPF pressues, are sensitive to variations of the orientation of the fibers $\pm\theta$. In particular, the BB pressures tend to increase when θ increases from 20° to 90°, for the cylinders reinforced with E-glass and carbon fobers, as illustrated in Figures 7 and 8. For the cylinders reinforced with E-glass fibers, Pb increases continuosly, as θ increases from 20° to 90°. And, for those reinforced with carbon, Pb increases continuosly, when θ increases from 20° to about 63° and then almost stabilises for $63° < \theta < 90°$.

The FPF pressures predicted using the failure criteria of Tsai-Hill and Hoffman were practically the same for the cylinders reinforced with E-glass fibers (see Fig. 5), whereas for those reinforced with carbon the failure criterion of Tsai-Hill was more conservative, for $40° < \pm \theta < 80°$, and practically identical to the criterion of Hoffman for all other orientations (see Fig. 6).

For the situations investigated on the present study, there were no cases in which axissimetric collapse (AC) or material failure controlled by Last Ply Failure (LPF) occurred before (i.e. at lower pressures) BB or FPF.

6. MAIN CONCLUSIONS

For the simulations carried out in this study, there was a clear indication that the cylinders reinforced with carbon fibers are stronger and present higher buckling pressures in comparison with those reinforced with E-glass. For both groups of cylinders, the geometry and the boundary conditions were exactly the same.

In all the simulations carried out so far, the most critical mode of failure was bifurcation buckling (BB), with the number of circumferential waves varying from 2 to 4. Since the cylinders evaluated in this study are typical thin shells, presenting R/t = 50, this is not a surprise.

7. ACKNOWLEDGEMENTS

The authors are grateful to the support received from CNPq and ELETRONORTE during all the execution of this investigation.

8. REFERENCES

Baldoino, W., M., "Simulação Numérica do Comportamento Mecânico de uma Barra de Material Compósito, Análise Estática e de Estabilidade", Dissertação de Mestrado, UnB, ENM, 1998.

Campestrini, E., A. e Sousa Moura, R. W.,1997, Análise de Tensões e Estabilidade em Cilindros de Material Compósito Submetidos a Esforços Combinados, Relatório de Estágio Supervisionado, Universidade de Brasília, Brasília.

Daniel, I.M. and Ishai, O. (2006), Engineering Mechanics of Composite Materials, Oxford University Press, Oxford.

Gibson, R.F., (1994), Principles of Composite Materials Mechanics, Mc Graw-Hill Inc., New York.

Gonçalves, A., Almeida, S.F.M., and Levy Neto, F., 2001, "Comportamento de Cilindros de Carbono/Epóxi Submetidos a Cargas Compressivas Axiais", Polomeros: Ciência e Tecnologia, No. 2, Vol. XI, pp. 94 - 101

Hoa, S. V. (1991), Analysis for Design of Fiber Reinforced Plastic Vessels and Piping. Technomic, Lancaster.

Hull, D And Clyne, T. W., 1996, An Introduction to Composite Materials, Cambridge Univerity Press, Cambridge.

Levy Neto, F., 1991, The Behavior of Externally – Pressurised Composite Domes, Liverpool, PhD. Thesis, University of Liverpool 1991.

Ross, C.T.F., 1990, "Pressure Vessels under External Pressure – Static and Dynamics", Elsevier, London.

Tsai, S. W., Composite Design, Think Composite, Dayton, 1987.

9. RESPONSIBILITY NOTICE

The authors are the only responsible for the printed material included in this paper.